P3R.3 INTERCOMPARISONS OF NOWCASTING TECHNIQUES

Steven A. Lack *
Neil I. Fox
David M. Jankowski
George L. Limpert
University of Missouri-Columbia,
Columbia, Missouri, USA

1. INTRODUCTION

As the science of nowcasting continues to advance there is the need for comparison between multiple systems to show their respective strengths and weaknesses. In this paper two such systems will be examined and a third experimental system will be introduced. The two systems involve a centroid-type nowcast scheme (SCIT) versus a correlation-type nowcast scheme (S-PROG). The situations examined for this study involve the formation of a mesoscale convective system (MCS) on 15 June 2002 near Goodland, KS and the 5 May 2003 tornado outbreak near Springfield, MO. Although the comparison of forecast tracks is rather simplistic a new method of real-time verification will be revealed.

2. METHODOLOGY

For simplicity of comparison, the differences in the nowcasts are displayed as differences of the actual storm motion vectors from the forecasted storm motion vector of the given nowcast scheme. The actual storm motion vectors are calculated from the given coordinates of the identified centroid location in the storm cell identification and tracking algorithm as used in the research version of WDSS-II. A rear-edge storm motion vector will also be compared to the nowcasts for completeness. This comparison is done for a 5, 30 and 60 minute nowcast from an initial start time. For simplicity the motion vectors (actual and forecast) are broken up into direction and speed.
The two nowcasting schemes will be explained briefly below.

* *Corresponding author address:* Steven A. Lack, Univ. of Missouri-Columbia, Dept. of SEAS, Columbia, MO 65211-1234; e-mail: SALack@mizzou.edu.

2.1 *SCIT*

SCIT (Storm Cell Identification and Tracking) is a centroid-based nowcasting system that uses seven reflectivity thresholds to determine a cell position and then extrapolate a storm track using an equal-weighted track history (Johnson et al., 1998). In this study the centroid location and the forecast vector were recorded and then compared using simple trigonometry. One advantage of SCIT is that cells identified have different forecast directions and speeds and can be allowed to converge and intensify or diverge and dissipate. A disadvantage to SCIT in this study is to find cells that are consistently identified for one hour. In some cases, the cell may change identification and the nearest identified cell may not result in an accurate propagation estimation of what appears to be a continuous storm.

2.2 *S-PROG*

S-PROG is a spectral decomposition model which uses scale dependent temporal evolution to formulate forecasts (Seed, 2003). The usefulness of such a decomposition model is that it allows for a degree of implicit uncertainty in the final rainfall nowcast. The uncertainty is based on the residency time of features at certain spatial scales; the larger spatial features last longer. The advection of the system as a whole utilizes correlation techniques. This correlation technique results in an x and y coordinate translation based on pixel size for one forecast solution set. These coordinates are then converted to speed and direction components for easy comparison to actual and SCIT forecasts.

2.3 *Rear-edge Motion*

Storm velocities are generally calculated by using the center of the storm. This calculation may lead to a better understanding of when a storm will reach a location, but may be misleading when it comes to the lingering effects of storm cells. This rear-edge can be located by using the storm track and following it from the centroid to the rear of the storm cell using 30 dBZ as a threshold. Once the rear-edge is identified in consecutive scans a motion vector can be determined. The rear edge is compared to the nowcasts in this research to examine if a nowcast may capture the rear edge velocity better than the actual velocity calculated from consecutive positions of the centroid. If this is the case, the nowcast may handle quantitative precipitation for flooding applications effectively for certain modes of convection. For a more complete discussion of rear-edge velocities see Fox *et al*. (2005).

3. RESULTS

3.1 *Motion Vector Comparison*

The first case examined deals with a developing mesoscale convective system (MCS) under the Goodland, KS radar umbrella on 15 June 2002. This event produced severe hail and wind and significant rainfall in western Kansas. The case examined deals with the development of a potentially severe storm to the west of the radar (see Fig. 1, 2). Table 1 includes an example of the numerical motion vectors over 5-min, 30-min, and 60-min found from both the centroid and rear-edge tracking schemes compared to the initial SCIT and S-PROG forecast motion from the initial time of 17:13Z.

In this case of the developing cell the velocity forecast by S-PROG is consistently closer to the rear-edge velocity diagnosed than to the centroid velocity. This is probably due to the dispersion of the cell area as it develops combined with the reflectivity distribution that locates the high reflectivity core, and therefore the centroid, toward the rear of the cell.

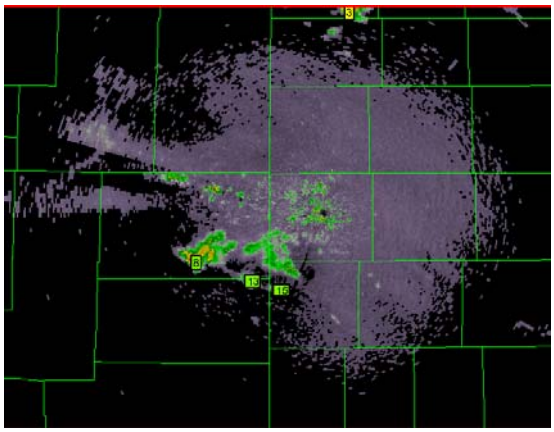

Figure 1. Reflectivity with SCIT identification tags from 15 June 2002 at 17:13Z, the cell of interest is currently southwest of KGLD.

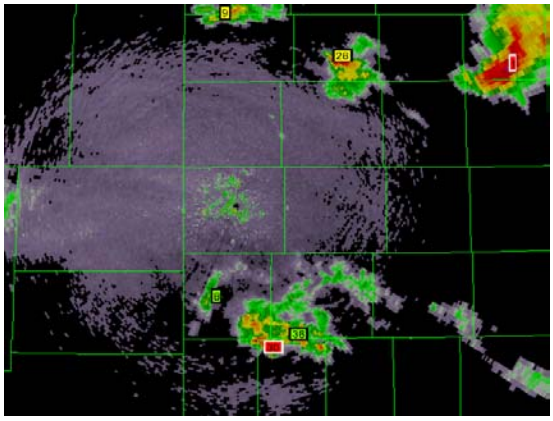

Figure 2. Reflectivity with SCIT identification tags from 15 June 2002 at 18:13Z, the cell of interest is currently south-southeast of KGLD.

Initial Time	Direction	Speed (m/s)	Product
17:13Z	304.00	14.000	SCIT
17:13Z	291.57	14.079	S-PROG
Time Step	**Direction**	**Speed (m/s)**	**Product**
5-min	283.55	20.608	Centroid
30-min	288.32	17.099	Centroid
1 hour	294.46	17.709	Centroid
5-min	260.82	12.251	Rear-edge
30-min	286.66	16.233	Rear-edge
1 hour	293.92	17.674	Rear-edge

Table 1. The forecast motion vectors versus the actual motion vectors storm cell FILL IN.

The other case examined was from the 5 May 2003, during the May Tornado Outbreak of 2003. This supercellular case was selected because there were many merging storm cells that contributed to the formation of powerful tornadoes across Kansas and Missouri. The cells with SCIT identification tags as displayed by WDSS-II can be seen in Figs 3 and 4.

Table 2 includes the numerical motion vectors over 5-min, 30-min, and 60-min derived from the centroid and rear-edge tracking schemes compared to the initial SCIT and S-PROG forecast motion from the initial time of 00:13Z, cell number 1 (66 at later time steps). Motion vectors are given in (a) and cell number 2 motion vectors are given in (b).

(a)

Initial Time	**Direction**	**Speed (m/s)**	**Product**
00:13Z	265.00	22.500	SCIT
00:13Z	248.25	26.417	S-PROG
Time Step	**Direction**	**Speed (m/s)**	**Product**
5-min	261.38	26.193	Centroid
30-min	256.45	20.781	Centroid
1 hour	256.49	19.995	Centroid
5-min	254.73	21.002	Rear-edge
30-min	252.50	20.021	Rear-edge
1 hour	252.58	21.368	Rear-edge

(b)

Initial Time	**Direction**	**Speed (m/s)**	**Product**
00:13Z	249.00	14.800	SCIT
00:13Z	248.25	26.417	S-PROG
Time Step	**Direction**	**Speed (m/s)**	**Product**
5-min	240.98	17.526	Centroid
30-min	251.34	20.353	Centroid
1 hour	250.43	20.416	Centroid
5-min	242.70	29.758	Rear-edge
30-min	254.02	22.748	Rear-edge
1 hour	245.77	23.478	Rear-edge

Table 2. The forecast motion vectors versus the actual motion vectors for both storm cell number 1 (66 in later images) (a) and storm cell 2 (b).

From the data in table 2, it can be shown that, for the supercellular case, the rear-edge motion of the storm shows no consistent trend, as it is slower in general than the centroid motion for the southerly cell, but faster than the centroid motion in the northerly cell. These results are to be expected from results compiled by Fox *et al.* (2005). The comparisons in this case seem to be better for the SCIT forecast results as it tends to pick up the movement to the right of the supercell whereas S-PROG tends to pick up the mean motion of the system as a whole governed by the less severe larger features, which is also expected due to the architecture of the S-PROG scheme. Although the forecast speed tends to be faster than the actual motion of both the rear-edge and centroid this is not terrible for this severe weather situation. The potential increase in lead-time in issuing a county-based tornado warning if the forecast is slightly fast can actually be beneficial.

The data that is not shown by this table are the values of the SCIT and S-PROG forecasts after the initial time steps. The trend in the forecast from SCIT shows the tendency toward right movement while the supercells are reaching maturity, followed by the trend toward the mean motion as the cells decrease in intensity. This follows quite well in the physical sense.

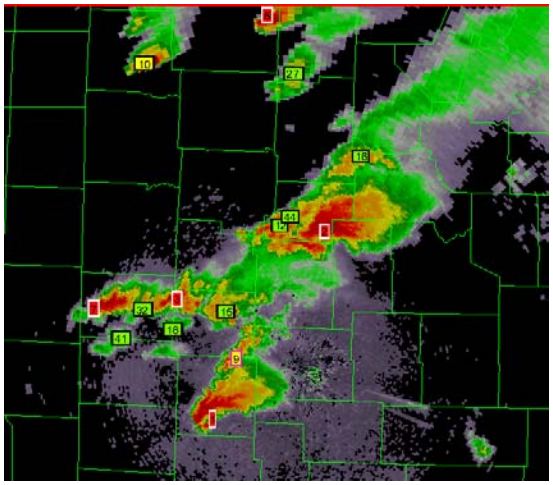

Figure 3. Reflectivity with SCIT identification tags from 5 May 2003 at 00:13Z, cell 1 in the southern portion of the image is the Pierce City Tornado; the other cell examined is cell 2 toward the center of the image.

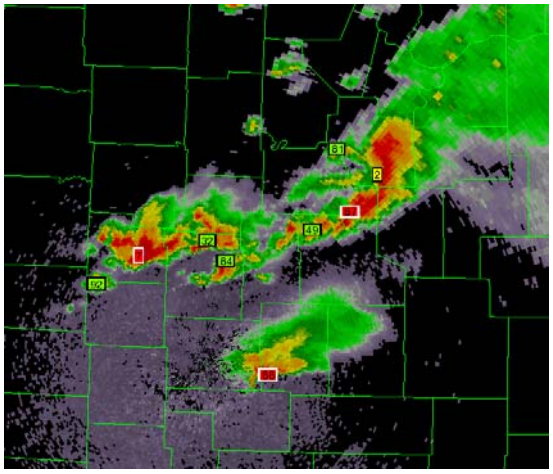

Figure 4. Reflectivity with SCIT identification tags from 5 May 2003 at 0113Z, cell 66 in the southern portion of the image is the remnants of the Pierce City Tornado; the other cell examined is cell 2 toward the center of the image.

3.2 *Pseudo-Radar Image Comparison*

One of the most useful aspects of both the WDSS-II system and S-PROG is the pseudo-radar image it produces for each forecast. For this study, both S-PROG and WDSS-II were run to produce images for 30 and 60 minute forecasted time steps. The most notable difference is how each scheme creates its forecast. S-PROG uses a spatial cascade approach as described by Seed (2003), while WDSS-II utilizes a K-Means approach described by Lakshmanan et al. (2003). The general idea behind this approach, as outlined by Lakshmanan *et al.* (2003), is to find storms at different scales, estimate the motion vectors at these various scales, and produce a forecast using this information. The radar data may be used in conjunction with satellite data; however for the cases presented here satellite data was excluded. Again, the WDSS-II forecast allows identified cells to move independently of other cells, whereas, S-PROG uses one generalized motion vector.

Figures 5-9 are the 30- and 60-minute forecasts and actual radar images for comparison from the 5 May 2003 case initializing at 00:13Z. The 30-minute S-PROG forecast seems to pick up most of the major features and even retains the hook echo to some degree; however, the forecast speed appears to be faster than the actual.

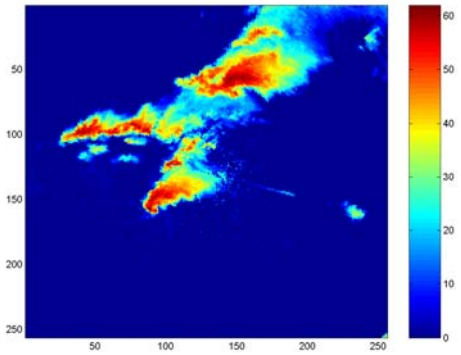

Figure 5. Initialization for 0013Z 5 May 2003 at the KSGF radar. Color scale is in dBZ.

The 1-hr S-PROG forecast is quite different than the actual as S-PROG smoothes and spreads out the higher reflectivity core. The 1-hr forecast also fails to capture the redevelopment along the flank of the northern cells, yielding a poor skill score (Table 3).

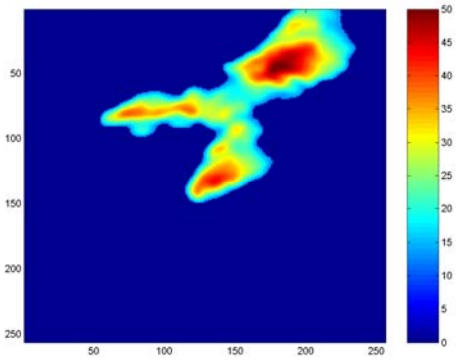

Figure 6. 30-minute S-PROG forecast from KSGF at 0013Z 5 May 2003 valid for 0043Z 5 May 2003 .

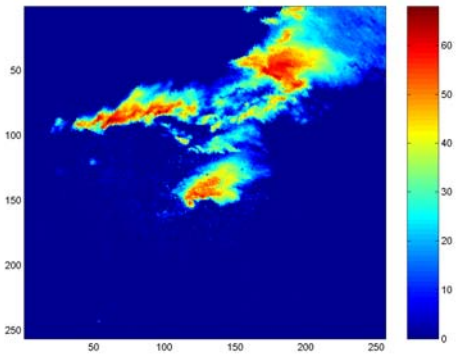

Figure 7. Actual radar image for 0043Z 5 May 2003 KSGF.

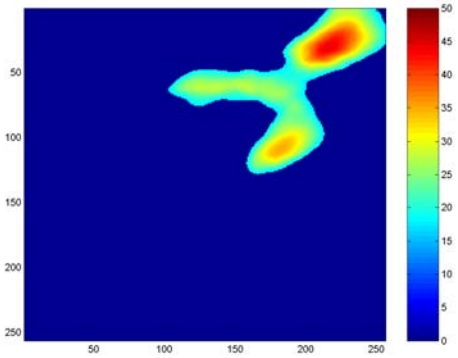

Figure 8. 60-minute S-PROG forecast from KSGF at 0013Z 5 May 2003 valid for 0113Z 5 May 2003.

On the other hand, the WDSS-II K-Means method of nowcasting produces images that yield quite high skill scores (Table 3). Both S-PROG and WDSS-II capture the southern cell quite well; however, WDSS-II does a better job with the northern cell and the redevelopment along the rear of the initial intense supercell (Fig 10-11). Since the WDSS-II nowcast provides a growth and decay element it is no surprise

that it would handle a long-lived supercell event with little to no loss of high reflectivity cores.

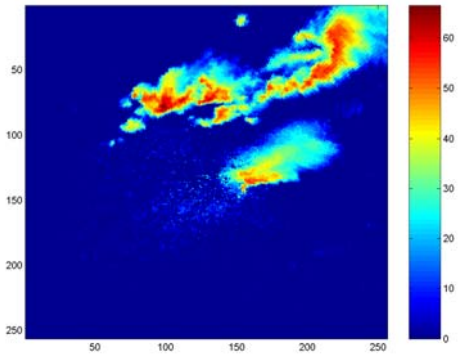

Figure 9. Actual radar image for 0113Z 5 May 2003 KSGF.

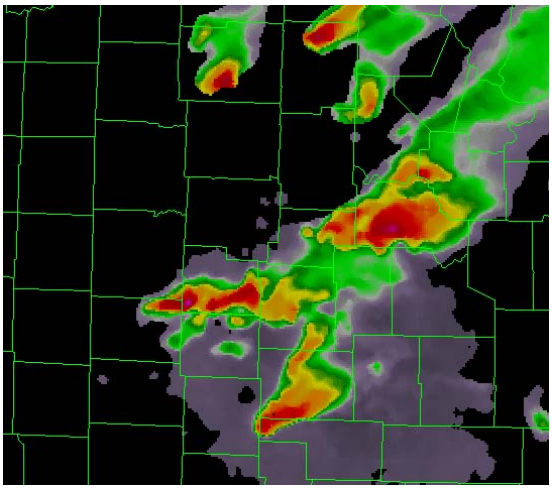

Figure 10. 30-minute WDSS-II forecast from 0013Z valid 0043Z KSGF.

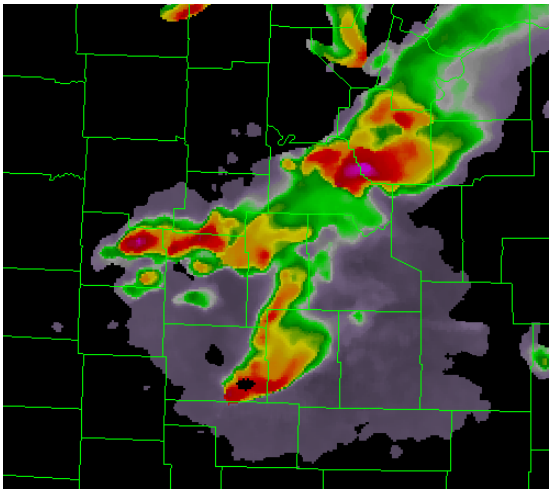

Figure 11. 60-minute WDSS-II forecast from 0013Z valid 0113Z KSGF

The next group of figures (12-16) is the S-PROG output from the 15 Jun 2002 case over the KGLD radar site. This is a more linear MCS-type case where the uniform motion vector calculated by S-PROG was fairly accurate. However, the skill scores (Table 3) for this case are quite poor, and are perhaps misleading. The isolated nature of the cells within the domain causes a smoothing out to below the threshold used for skill scoring after the S-PROG scheme is applied. The threshold has to be reduced substantially to yield a probability of detection above zero. Again, WDSS-II (Fig. 17-18) outperforms S-PROG in terms of skill scores; however, the implicit uncertainty in S-PROG still makes it highly applicable.

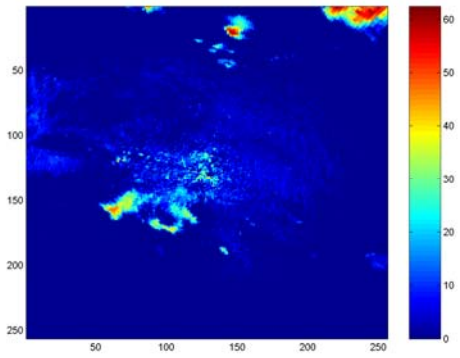

Figure 12. Initialization for 1713Z 15 June 2002 KGLD.

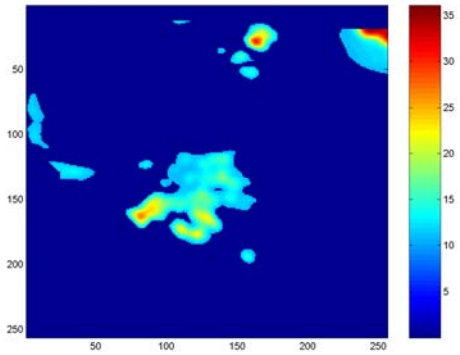

Figure 13. 30-minute S-PROG forecast from KGLD at 1713Z 15 June 2002 valid for 1743Z 15 June 2002

In summary, it can be shown that although the WDSS-II forecast product utilizing the K-Means method outperforms S-PROG in terms of spatial skill scores (Table 3), S-PROG can be a useful nowcaster, especially when running S-PROG in an ensemble framework (Pierce *et al*. 2005). S-PROG picks up mean motions of precipitation areas quite well, despite its large domain.

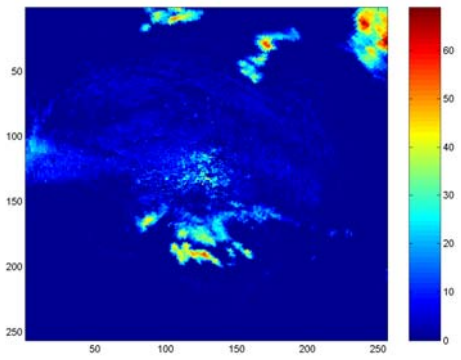

Figure 14. Actual radar image for 1743Z 15 June 2002 KGLD.

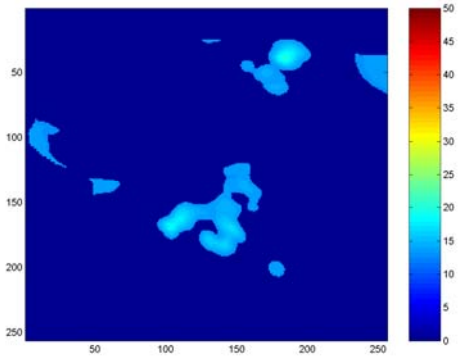

Figure 15. 60-minute S-PROG forecast from KGLD at 1713Z 15 June 2002 valid for 1813Z 15 June 2002.

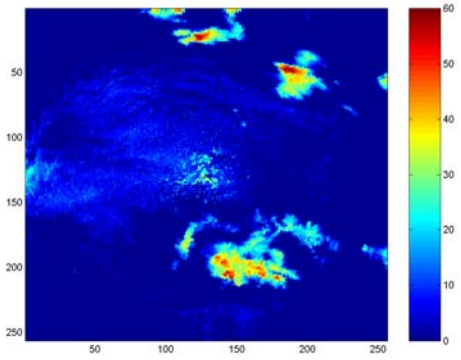

Figure 16. Actual radar image for 1813Z 15 June 2002 KGLD.

It will have problems when new cells are developing throughout the domain, but on the whole it will pick up the background flow for the domain, which can be quite useful. S-PROG's implicit uncertainty recognizes the fact that high intensity small scale features have short residency times. However, in self-sustaining supercells this approach appears weak. One known problem alluded to by Lakshmanan et al. (2003) is that although it may score highly with respect to CSI; the intensity forecast can be off significantly. Overall, S-PROG may be best applied to uniform areas of non-severe convection, whereas the centroid-based nowcaster (WDSS-II, SCIT) may handle severe weather better. In addition, the cell attribute tables generated by the centroid-based nowcasters have proven to be invaluable.

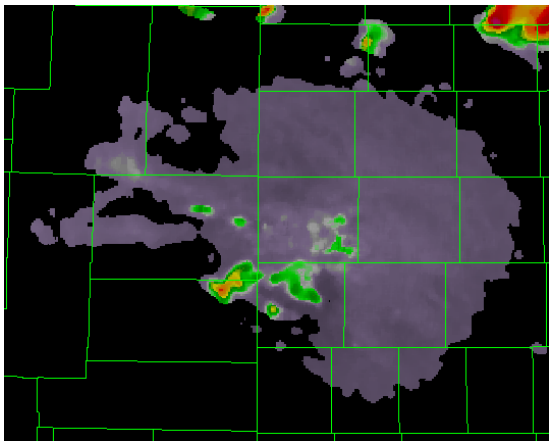

Figure 17. 30-minute WDSS-II forecast from 1713Z valid 1743Z KGLD.

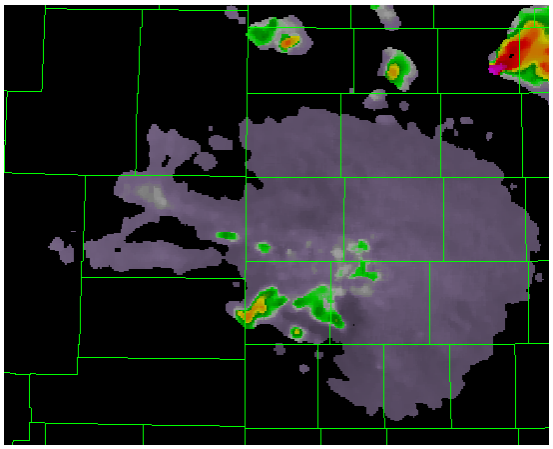

Figure 18. 60-minute WDSS-II forecast from 17:13Z valid 1813Z KGLD.

Inter.	Case	Scheme	POD	FAR	CSI
30 min	5-May-03	S-PROG	0.68	0.21	0.58
30 min	5-May-03	WDSS-II	0.88	0.27	0.66
60 min	5-May-03	S-PROG	0.51	0.28	0.42
60 min	5-May-03	WDSS-II	0.73	0.35	0.52
30 min	15-Jun-02	S-PROG	0.37	0.36	0.30
30 min	15-Jun-02	WDSS-II	0.84	0.19	0.70
60 min	15-Jun-02	S-PROG	0.10	0.69	0.08
60 min	15-Jun-02	WDSS-II	0.70	0.26	0.56

Table 3. Skill Score comparison between Sprog and WDSS-II forecasts using 20 dBZ as the threshold.

4. NEW REAL-TIME VERIFICATION METHODS

Although skill scores such as POD, FAR, and CSI are useful, especially in post-analysis, there is a need for real-time verification so a forecaster can see immediate biases in products. Currently a scheme is being designed to create a scoring method that could provide a plethora of information to an end user by real-time image comparison. Using Procrustes techniques for shape analysis, we should be able to produce real-time verifications for any nowcast that produces a forecast radar image. The shape analysis performed by the Procrustes scheme can be broken down into several components so that users may see biases in the model in near real-time and adjust the forecast as necessary. This information could provide useful information for applications from severe weather forecasting to hydrologic applications where model uncertainty can be used to predict streamflow.

5. ACKNOWLEDGEMENTS

This work was funded, in part, by National Science Foundation grant DMS-0139903. WDSS-II has been developed jointly by engineers and scientists at the National Severe Storms Laboratory (NSSL) and the Cooperative Institute of Mesoscale Meteorological Studies (CIMMS) at the University of Oklahoma and we thank Dr. Lakshmanan for assistance. S-PROG was developed at the Bureau of Meteorology Research Centre, Australia and we thank Alan Seed for providing us with the software and all his help.

6. REFERENCES

Fox, N.I., D.M. Jankowski, E.A. Hatter and E. Heiberg, 2005: Forecasting storm duration, Preprints: World Weather Research Programme's symposium on nowcasting and very short range forecasting, Toulouse, France, 5-9 September, 2005.

Johnson, J.T., P.L. MacKeen, A. Witt, E.D. Mitchell, G.J. Stumpf, M.D. Eilts, K.W. Thomas, 1998: The storm cell identification and tracking algorithm: an enhanced WSR-88D algorithm. *Wea. Forecasting*, **13**, 263-276.

Lakshmanan, V., R. Rabin, and V. DeBrunner, 2003: Multiscale storm identification and forecast. *Atmos. Research*, **67-8**, 367-380.

Pierce, C. N. Bowler, A. Seed, A. Jones, D. Jones, and R. Moore, 2005: Use of a stochastic precipitation nowcast scheme for fluvial flood forecasting and warning. *Atmos. Sci. Lett*., **6**, 78-83.

Seed, A.W, 2003: A dynamic and spatial approach to advection forecasting. *J. Appl. Meteor*., **42**, 381-388.